

Lattice Regularization of Non-relativistic Interacting Fermions in One Dimension

Zihan Li^{a)} and Son T. Nguyen^{b)}

*Department of Physics and Engineering, Washington and Lee University,
Lexington 24450, USA*

(Dated: January 6, 2026)

Few-body physics plays a central role in many branches of physics, such as nuclear physics and atomic physics. Advances in controlling ultra-cold quantum gases provide an ideal testbed for few-body physics theory. In this work, we study few-body systems consisting of two distinct species of non-relativistic fermion in one spatial dimension using both field theory and lattice methods. Particles of the same type do not interact with each other, but particles of different type can interact via an attractive contact interaction. We first study the dependence of the coupling of a contact interaction on the lattice spacing. Using this input, we extract two-, three- and four-body's ground state energies in the infinite length limit and benchmark them against the calculations from the continuum field theory. This work enables us to systematically study the effect of discretization and finite-length artifacts on few-body observables.

^{a)}Electronic mail: zli@mail.wlu.edu

^{b)}Electronic mail: snguyen@mail.wlu.edu

I. INTRODUCTION

Ultracold Fermi gases have been the subject of extensive experimental studies due to their high degree of tunability by applying external magnetic fields and leveraging Feshbach resonances and their role as clean realizations of strongly interacting quantum systems^{1–6}. In the low-energy limit, the physics of interacting fermions becomes universal, as the detailed microscopic structure of the interaction is integrated out^{7–9}. In the continuum, fermionic systems with short-range interactions are therefore well described by effective models with contact interactions.

For two-component fermions in one dimension (1D), this universality leads to the Gaudin-Yang model^{10,11}, which provides the continuum description of fermions interacting via a delta potential. The Gaudin-Yang model is one of the most important exactly solvable quantum many-body systems. The model can be solved exactly using the Bethe ansatz, which has been successfully implemented to obtain the ground-state energy, excitation spectrum, and thermodynamic properties in the continuum. These exact solutions have played a central role in establishing our understanding of correlation effects, pairing phenomena, and crossover from the Bardeen-Cooper-Schrieffer (BCS) state of weakly-correlated pairs of fermions to the Bose-Einstein condensation (BEC) of diatomic molecules in one-dimensional fermionic systems (see e.g., Ref.¹² for a comprehensive review). While the Bethe ansatz provides an exact solution for the model, it relies on the assumption of non-diffractive, factorized scattering. In the presence of mass imbalance, this assumption is generically violated, leading to diffractive multi-particle scattering and the breakdown of integrability^{13–15}.

In this work, we study few-body fermionic systems in 1D with attractive contact interactions using both field theoretic and lattice methods. The former enables the direct and systematic calculation of few-body bound states and scattering properties. The latter can provide a non-perturbative computation framework by putting these fermions on a discretized space (and time if needed).

From the field theoretic perspective, we calculate the two-body scattering amplitude using the dimer formalism¹⁶ and recover the standard result that the contact interaction does not require regularization in 1D. For attractive coupling, we reproduce the single two-body bound state, which agrees with the quantum mechanics of the delta potential. Then following the method outlined in Ref.¹⁶ for a three-body system, we can derive the Skornyakov-Ter-

Martirosyan (STM) integral equation for fermion-dimer scattering and confirm that there is no new three-body bound state (trimer) in 1D. It is worth mentioning that in three dimensions the corresponding STM equation admits qualitatively different behavior, including the existence of nontrivial three-body bound states^{17–19}. As far we know, the four-body problem for one-dimensional fermions with contact interactions remains an active area of research^{20,21}.

Lattice method is a natural tool for considering larger system and can be adjust to include, for example, repulsive interactions among fermions and mass-inbalance. Lattice calculations are usually performed in a discretized finite box with periodic boundary conditions. We first recast the two-component fermions Lagrangian in the lattice Hamiltonian language. In contrast to the continuum theory, the coupling is actually regulated by the lattice spacing. We study the continuum limit of two-body observables analytically and verify those results with exact diagonalization and another finite-length method²². Once the Hamiltonian and the coupling are specified, we can compute the spectrum of three-and four-body systems exactly.

By varying the box size, one can isolate finite-volume effects and extrapolate results to the infinite-volume limit. In low-energy systems, these corrections are often governed by universal forms determined by the asymptotic structure of bound states or scattering amplitudes^{23–25}. Again, in the two-body sector, we show that the ground state’s binding energy can be reproduced precisely in both continuum and infinite length limits. Errors due to lattice artifacts are carefully scrutinized. Nonetheless, we observed that these errors are prominent in higher-body sectors, resulting in the disagreement between finite-length calculations and continuous theory’s expectations. The limitations in accessible finer lattice spacings and larger box sizes restrict the precision of extrapolations. On the other hand, the resulting calculations still offer valuable qualitative and semi-quantitative insight into the structure of few-body systems and the role of lattice artifacts. Additionally, they can be used as benchmarks for developing novel many body computational techniques, including Monte Carlo sampling and tensor-network methods.

Although we focuses on one-dimensional systems in this work, the lattice and finite-volume methods employed here are closely connected to techniques widely used in three-dimensional nuclear and cold-atom physics. In particular, few-body nuclear observables and their volume dependence are routinely used in three dimensions to study bound states

and scattering^{26,27}. On the other hand, the lattice formalism itself provides an *ab initio* framework to study finite-volume effect which enables making predictions for few- and many-body nuclear systems²⁸. One-dimensional systems often capture universal aspects of short-range interactions and few-body dynamics that persist beyond a specific dimensionality^{29–32}. In this sense, one-dimensional models provide a perfect testbed for understanding lattice artifacts and finite-volume effects, offering valuable insights relevant in higher dimensions.

Our work is organized as follows. In Section II, we revisit the delta potential problem from the quantum field theory perspective. A different approach to solving the same system via lattice regularization is in Section III. This section includes details of studying a system on a lattice and compares results with other methods. Section IV presents an infinite volume extrapolation based on the lattice system. Section V is a brief conclusion of our work.

II. FIELD THEORY PERSPECTIVE

We consider a one-dimensional system of two-component fermions with attractive zero-range interactions. The Lagrangian is given by

$$\mathcal{L} = \sum_{\sigma=1,2} \psi_\sigma^\dagger \left(i\partial_0 + \frac{\partial_x^2}{2m_\sigma} \right) \psi_\sigma - U\psi_1^\dagger\psi_2^\dagger\psi_2\psi_1, \quad (1)$$

where ψ_1 and ψ_2 are two species of non-relativistic particles living in one spatial dimension, U is unknown parameters of the theory. The Hamiltonian associated with this system reads

$$H = \sum_{\sigma=1,2} -\frac{1}{2m_\sigma} \psi_\sigma^\dagger \partial_x^2 \psi_\sigma + U(\psi_2\psi_1)^\dagger\psi_2\psi_1, \quad (2)$$

which is commonly referred to as the Yang-Gaudin model^{10,11}. The Bethe ansatz solutions for three- and four-body systems can be found in, e.g., Refs.^{9,33} and references therein.

For convenience of diagrammatic calculations in three-body sector, we introduce a auxiliary dimer fields ϕ ,

$$\begin{aligned} \mathcal{L} = & \sum_{\sigma=1,2} \psi_\sigma^\dagger \left(i\partial_0 + \frac{\partial_x^2}{2m_\sigma} \right) \psi_\sigma + \Delta_\phi \phi^\dagger \phi \\ & - g_1 (\phi^\dagger \psi_2 \psi_1 + \text{H.c.}) \end{aligned} \quad (3)$$

The equation of motion for the auxiliary field is

$$\Delta_\phi \phi - g_1 \psi_2 \psi_1 = 0, \quad (4)$$

Bringing the solution for ϕ back to the Lagrangian with auxiliary fields, we can rewrite the interaction coefficient U as

$$U = \frac{g_1^2}{\Delta_\phi}. \quad (5)$$

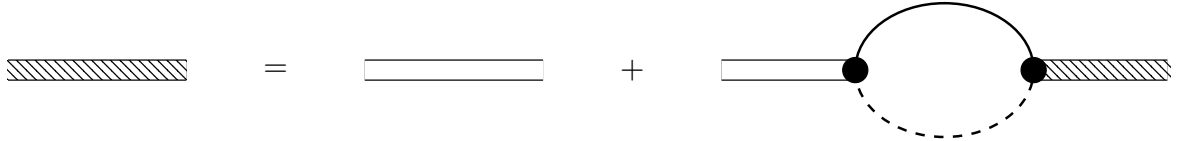


FIG. 1: The dimer field's dressed propagator. The thick empty double line denotes the bare propagator. The solid line represents ψ_1 's propagator while the dashed line represents ψ_2 's propagator. The black circle indicates the insertion of the g_1 vertex.

The propagator of the ψ_σ field is $iD_\sigma(E, p) = i/(E - p^2/2m_\sigma + i\epsilon)$, while the bare propagator of the dimer field ϕ is $iD_\phi^{(\text{bare})} = -i(\Delta_\phi + i\epsilon)^{-1}$. For simplicity, we assume that $m_1 = m_2 = m$. In this formalism, we can find the dressed propagator (see Fig. 1) by solving the following equation

$$iD_\phi = iD_\phi^{(\text{bare})} + iD_\phi^{(\text{bare})}(-ig_1)^2 \mathcal{I}_0 iD_\phi. \quad (6)$$

It follows that

$$iD_\phi = \frac{i}{\left[D_\phi^{(\text{bare})}\right]^{-1} + i g_1^2 \mathcal{I}_0}, \quad (7)$$

where \mathcal{I}_0 is the irreducible self-interaction loop integral given by

$$\begin{aligned} \mathcal{I}_0(p_0, p) &= \int \frac{dq_0 dq}{(2\pi)^2} iD_{\psi_1}(q_0, q) iD_{\psi_2}(p_0 - q_0, p - q) \\ &= i \int \frac{dq}{2\pi} \frac{1}{p_0 - \frac{(q-p/2)^2}{m} - \frac{p^2}{4m} + i\epsilon} \\ &= -i \frac{m}{2} \frac{1}{\sqrt{p^2/4 - mp_0 - i\epsilon}}. \end{aligned} \quad (8)$$

Thus, substituting Eq. (5) and Eq. (8) into Eq. (7) gives

$$iD_\phi(p_0, p) = \frac{i}{\Delta_\phi} \frac{1}{1 + \frac{mU}{2\sqrt{p^2/4 - mp_0 - i\epsilon}}}. \quad (9)$$

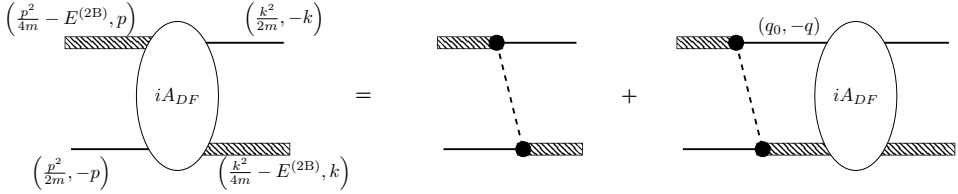


FIG. 2: Feynman diagrams contributing to the fermion-dimer scattering amplitude.

The resulting loop integral is finite and independent of the regularization scheme. The two-body scattering amplitude in the center of mass (c.o.m) frame is

$$iA_{2B}(E) = (-ig_1)^2 iD_\phi(E, 0) = \frac{-iU}{1 + \frac{iUm}{2\sqrt{mE}}}. \quad (10)$$

The contact coupling U is a constant parameter. The scattering amplitude has a pole at $E = -E^{(2B)} = -mU^2/4$, which reproduces the binding energy of the potential $V(x) = -U\delta(x)$ ³⁴.

Next, we consider the three-body system consisting of two ψ_1 particles and one ψ_2 particle. In particular, we are interested in the scattering of ψ_1 of the dimer ϕ , which is pictorially represented in Fig. 2. Our choice of the kinematics is also described on Fig. 2 to form the half off-shell amplitude. We denote the sum of those diagrams by $a(p, k)$ and derive the following integral equation,

$$\begin{aligned} ia(p, k) &= ig_1^2 B(p, k) \\ &+ (-ig_1)^2 \int \frac{dq_0 dq}{(2\pi)^2} iD_\phi(E - q_0, q) iD_{\psi_1}(q_0, -q) \\ &\quad \times iD_{\psi_2} \left(E - \frac{p^2}{2m} - q_0, p + q \right) ia(q, k), \end{aligned} \quad (11)$$

where the nonhomogeneous term is given by

$$B(p, k) = \frac{m}{p^2 + pk + k^2 - mE - i\epsilon}, \quad (12)$$

where $E = 3p^2/4m - E^{(2B)}$. The integrand over dq_0 has only one pole $q_0 = q^2/(2m) - i\epsilon$ in the lower half-plane of q_0 , yielding

$$\begin{aligned} a(p, k) &= g_1^2 B(p, k) \\ &- g_1^2 \int \frac{dq}{2\pi} B(p, q) D_\phi \left(E - \frac{q^2}{2m}, -q \right) a(q, k) \end{aligned} \quad (13)$$

Eq. (13) can be solved numerically using Hetherington-Schick method³⁵. To obtain the dimer-fermion scattering amplitude $A_{DF}(p)$, we must multiply the on-shell amplitude $a(p, p)$ by the wave function renormalization factor,

$$A_{DF}(p) = \sqrt{\mathcal{Z}}a(p, p)\sqrt{\mathcal{Z}}, \quad (14)$$

with \mathcal{Z} being

$$\frac{1}{\mathcal{Z}} = \frac{\partial}{\partial E} \left[\frac{1}{D_\phi(E, 0)} \right] \Big|_{E=-E^{(2B)}} = \frac{2g_1^2}{mU^3}. \quad (15)$$

Without loss of generality, we can set $g_1^2 = 1$. If the three-body bound state exists such that $E = -\kappa^2/m$, the dimer-fermion scattering amplitude near that energy pole must behave like

$$a(p, k) \xrightarrow[E \rightarrow -\kappa^2/m]{} \frac{Z(p) Z^*(k)}{E + \kappa^2/m} + a_{\text{finite}}(p, k). \quad (16)$$

Taking residues on both sides of Eq. (13) with respect to $E = -\kappa^2/m$ gives

$$Z(p) = \int \frac{dq}{2\pi} B(p, q) D_\phi \left(E - \frac{q^2}{2m}, -q \right) Z(q). \quad (17)$$

We define $t(q) \equiv D_\phi \left(E - \frac{q^2}{2m}, -q \right) Z(q)$, we obtain the homogeneous integral equation for $t(q)$

$$\left(\frac{1}{U} + \frac{m}{\sqrt{3p^2 + 4\kappa^2}} \right) t(p) = -\frac{m}{2\pi} \int \frac{t(q) dq}{p^2 + pq + q^2 + \kappa^2} \quad (18)$$

The above equation has one analytical solution^{36,37}

$$t(p) = \frac{1}{p(p^2 + \kappa^2)} \quad (19)$$

with $\kappa = mU/2$, implying that the three-body system has an energy $E^{(3B)} = -mU^2/4$, which is identical to the binding energy of the two-body subsystem. This result indicates that there is no new three-body bound state. The third particle acts as a spectator, remaining asymptotically decoupled from the bound two-body subsystem. This is a well-known fact from studying the Gaudin-Yang model³³. This has been shown explicitly in the continuum^{36,37}, which showed that the effective atom-dimer interaction remains repulsive for all interaction strengths.

There are two main configurations in the four-body sector: one consisting of three ψ_1 particles and one ψ_2 particle, denoted by (3+1), and the other consisting of two ψ_1 particles

and two ψ_2 particles, denoted by $(2+2)$. The absence of a three-body bound state prevents the formation of larger clusters and ensures that the four-body sector introduces no new low-energy scales. As a result, tetramer bound states are forbidden. The lowest $(3+1)$ threshold is set by the two-body binding energy, while the $(2+2)$ threshold coincides with twice the two-body binding energy. The latter has been considered in Refs.^{20,21}. To end this section, we want to mention that in Ref.³³, which studied this problem in the effective field theory language, true three-body and four-body bound states should be eliminated because they exist beyond the breakdown scale of the theory.

III. FINITE VOLUME METHOD

A. Lattice Model

We study the same delta potential problems with a lattice regularized system. Particles are only allowed to exist in certain positions in space, known as the lattice sites. There are two important variables for a lattice model: The number of lattice sites, L , and the spacing between two adjacent sites, the lattice spacing, a .

Our lattice model is constructed in the Fock space formulation, using fermionic annihilation and creation operators $\psi_{\sigma,x}$ and $\psi_{\sigma,x}^\dagger$ where x is the lattice site on a periodic one-dimensional spatial lattice with L sites, and $\sigma = 1, 2$ are the two different fermion species. The lattice Hamiltonian can be arranged in two parts: a free Hamiltonian representing the kinetic part, H_0 , and an interaction term, H_{int} , representing the onsite interaction

$$H_1 = H_0 + H_{\text{int}}^{(\lambda)}, \quad (20)$$

where

$$H_0 = \epsilon(a) \sum_{x,\sigma} (\psi_{\sigma,x}^\dagger \psi_{\sigma,x+\alpha} - 2\psi_{\sigma,x}^\dagger \psi_{\sigma,x} + \psi_{\sigma,x+\alpha}^\dagger \psi_{\sigma,x}) \quad (21)$$

$$H_{\text{int}}^{(\lambda)} = \epsilon(a) \lambda(a) \sum_x \psi_{1,x}^\dagger \psi_{1,x} \psi_{2,x}^\dagger \psi_{2,x}. \quad (22)$$

In these above equations $\epsilon(a)$ is a function of a that sets the overall energy scale. Its value is determined by setting the ground state energy of a free particle on a lattice, $E_{1,\text{lat}}^{(1\text{B})} = E_1^{(1\text{B})}$, where $E_1^{(1\text{B})}$ is the lowest non-zero energy of a single free particle in a periodic one-

m_{phy} (MeV)	L_{phy} (fm)	$E_L^{(2\text{B})}$ (MeV)
940	3.4	-10

TABLE I: Input parameters used in the test calculation.

dimensional box. The ground state energy of this continuous theory has the form

$$E_1^{(1\text{B})} = \frac{2\pi^2}{m_{\text{phy}}L_{\text{phy}}^2}. \quad (23)$$

In what follows, we append the subscript “phy” to physical parameters to distinguish them from lattice parameters. It is straightforward to obtain the lattice model’s energy spectrum by diagonalizing H_0 in momentum space, yielding

$$E_{k,\text{lat}}^{(1\text{B})} = 2\epsilon(a) \left[1 - \cos\left(\frac{2\pi ka}{L_{\text{phy}}}\right) \right], \quad (24)$$

where $k = 0, 1, \dots, L - 1$. Finally, setting $E_{1,\text{lat}}^{(1\text{B})} = E_1^{(1\text{B})}$ gives us the relationship between $\epsilon(a)$ and known variables

$$\epsilon(a) = \frac{\pi^2}{m_{\text{phy}}L_{\text{phy}}^2} \left[1 - \cos\left(\frac{2\pi a}{L_{\text{phy}}}\right) \right]^{-1}. \quad (25)$$

A free Hamiltonian is relatively easy to calculate analytically. However, when interactions are turned on, it is impossible to compute all the numbers by hand. It would be more efficient to use numerical algorithms instead. For the rest of this paper, we use QuSpin³⁸, an open source Python package for exact diagonalization calculation. Some key input parameters are listed in Table I.

B. Renormalization with a Two-Body System

The lattice model in Eq. (20) is known as the Hubbard model. In the naive continuum limit of the one-dimensional Hubbard model, the on-site interaction becomes a delta-function interaction. Starting from the lattice Hamiltonian, and taking the lattice spacing $a \rightarrow 0$ with the spatial coordinate $xa \rightarrow x$, the interaction term formally becomes

$$\frac{U_{\text{lat}}(a)}{a} \sum_x n_{1,x} n_{2,x} \rightarrow U \int dx \psi_1^\dagger(x) \psi_2^\dagger(x) \psi_2(x) \psi_1(x), \quad (26)$$

where $n_{\sigma,x} = \psi_{\sigma,x}^\dagger \psi_{\sigma,x}$. In one-dimension continuum, the contact interaction is ultraviolet (UV) finite and does not require renormalization. On the lattice, the lattice spacing acts as a UV regulator. At fixed a the bare coupling is independent of the finite size of the space. In the continuum limit, the lattice coupling approaches the continuum coupling, $\lim_{a \rightarrow 0} U_{\text{lat}}(a) = U$. Comparing Eq. (22) and the left hand side of Eq. (26), $U_{\text{lat}}(a) \equiv a \epsilon(a) \lambda(a)$.

We can find $\lambda(a)$ analytically using the method outlined in Ref.³⁹. We introduce a relative momentum q and relative position δ to reduce a two-body system into a one-body system. A complete set of two particles can be defined as:

$$|q, \delta\rangle = \frac{1}{\sqrt{L}} \sum_x \psi_{2,x}^\dagger \psi_{1,x+\delta}^\dagger e^{i(2\pi/L)qx} |0\rangle. \quad (27)$$

In this basis, the Hamiltonian is block diagonal in $|q\rangle$. Since the ground state will appear in the sector with $q = 0$, we can focus on that sector and denote $|\delta\rangle \equiv |q = 0, \delta\rangle$ for short. The action of the Hamiltonian in Eq. (20) on this state is

$$\begin{aligned} H_1 |\delta\rangle &= 2\epsilon(a) (2|\delta\rangle - |\delta - \alpha\rangle - |\delta + \alpha\rangle) \\ &\quad + \lambda(a)\epsilon(a)\delta_{\delta,0} |\delta\rangle. \end{aligned} \quad (28)$$

As in the continuous theory, we are interested in the pole of the system. The information of potential poles is stored in the Green function matrix $G(E, a) = (E - H_1)^{-1}$. To simplify the full Green function, we expand it with a free Hamiltonian's Green function matrix, $G_0 = (E - H_0)^{-1}$ via

$$\begin{aligned} G(E, a) &= G_0(E, a) \\ &\quad + 2\epsilon(a)\mathcal{G}(E, a)G_0(E, a)|\delta = 0\rangle\langle\delta = 0|G_0(E, a), \end{aligned} \quad (29)$$

where $\mathcal{G} = [(2/\lambda(a)) - I_{\text{lat}}^{(\lambda)}(E, a)]^{-1}$. The dimensionless lattice interaction parameter $\lambda(a)$ corresponds to $2/I_{\text{lat}}^{(\lambda)}$, where $I_{\text{lat}}^{(\lambda)}$ is given by

$$I_{\text{lat}}^{(\lambda)}(E, a) = \frac{1}{L} \sum_{n=0}^{L-1} \frac{1}{E/2\epsilon(a) - 2[1 - \cos(2\pi n/L)]}. \quad (30)$$

Since we are interested in the bound state, $E = E_L^{(2B)}$ is negative. Using the Poisson summation formula (see Appendix A for more detail), it is possible to show that for $a \ll 1$ while $La = L_{\text{phy}}$ is fixed,

$$I_{\text{lat}}^{(\lambda)}(a) = \frac{-1}{2a\gamma_L} \coth\left(\frac{\gamma_L L_{\text{phy}}}{2}\right), \quad (31)$$

where $\gamma_L = \sqrt{m_{\text{phy}}|E_L^{(2B)}|}$ is the binding momentum defined from the finite-length energy. To derive the above expression, we have already used the fact that $\lim_{a \rightarrow 0} \epsilon(a) = 1/(2m_{\text{phy}}a^2)$ and neglected terms of order $\mathcal{O}(a^2)$ and higher. Clearly, $\lim_{a \rightarrow 0} \lambda(a) = \lim_{a \rightarrow 0} 2/I_{\text{lat}}^{(\lambda)}(a) = 0$ in the continuum limit. On the other hand, in this limit, $U_{\text{lat}}(a)$ is given by

$$U_{\text{lat}}(a) = -\frac{2\gamma_L}{m_{\text{phy}}} \tanh\left(\frac{\gamma_L L_{\text{phy}}}{2}\right), \quad (32)$$

which is independent of a . Therefore, U_{lat} has a well defined limit as $a \rightarrow 0$. Using tested parameters listed in Table I, we obtain $U_{\text{lat}} = -0.140966$. We can independently verify this value via exact diagonalization. We increase the number of lattice sites L up to 1024 sites while keeping the physical length fixed at $L_{\text{phy}} = 3.4$ fm. By demanding that the ground state is -10 MeV for each lattice spacing, we extract the lattice-spacing dependence of the coupling U_{lat} . Indeed, as $a \rightarrow 0$ we find that the lattice coupling converges to the continuum value, $\lim_{a \rightarrow 0} U_{\text{lat}}(a) = -0.140966$ (see Fig. 3).

Moreover, we can derive a relation between the finite-length energy and its infinite-length limit in a form of a transcendental equation,

$$E_{\infty}^{(2B)} = E_L^{(2B)} \tanh^2\left(\frac{\sqrt{m_{\text{phy}}|E_L^{(2B)}|} L_{\text{phy}}}{2}\right). \quad (33)$$

This naturally raises the question of whether fixing the coupling from the ground state is sufficient to determine the excited-state spectrum. This question can be answered by comparison with the Lüscher approach for the same system considered in Ref.⁴⁰ considered. The Lüscher's quantization condition relates the physical scattering length, a_1 , to the energy spectrum of the system in a finite box of length L_{phy} . In particular, Ref.⁴⁰ obtained the following relationship

$$\frac{a_1}{L_{\text{phy}}} = \frac{1}{2\pi^2} S_1^{\circlearrowleft}(x), \quad (34)$$

where the dimensionless quantity x is defined as

$$x = \frac{m_{\text{phy}} E^{(2B)} L_{\text{phy}}^2}{4\pi^2}. \quad (35)$$

The function $S_1^{\circlearrowleft}(x)$ has a known analytic form⁴⁰:

$$S_1^{\circlearrowleft}(x) = -\pi \frac{\cot(\pi\sqrt{x})}{\sqrt{x}}. \quad (36)$$

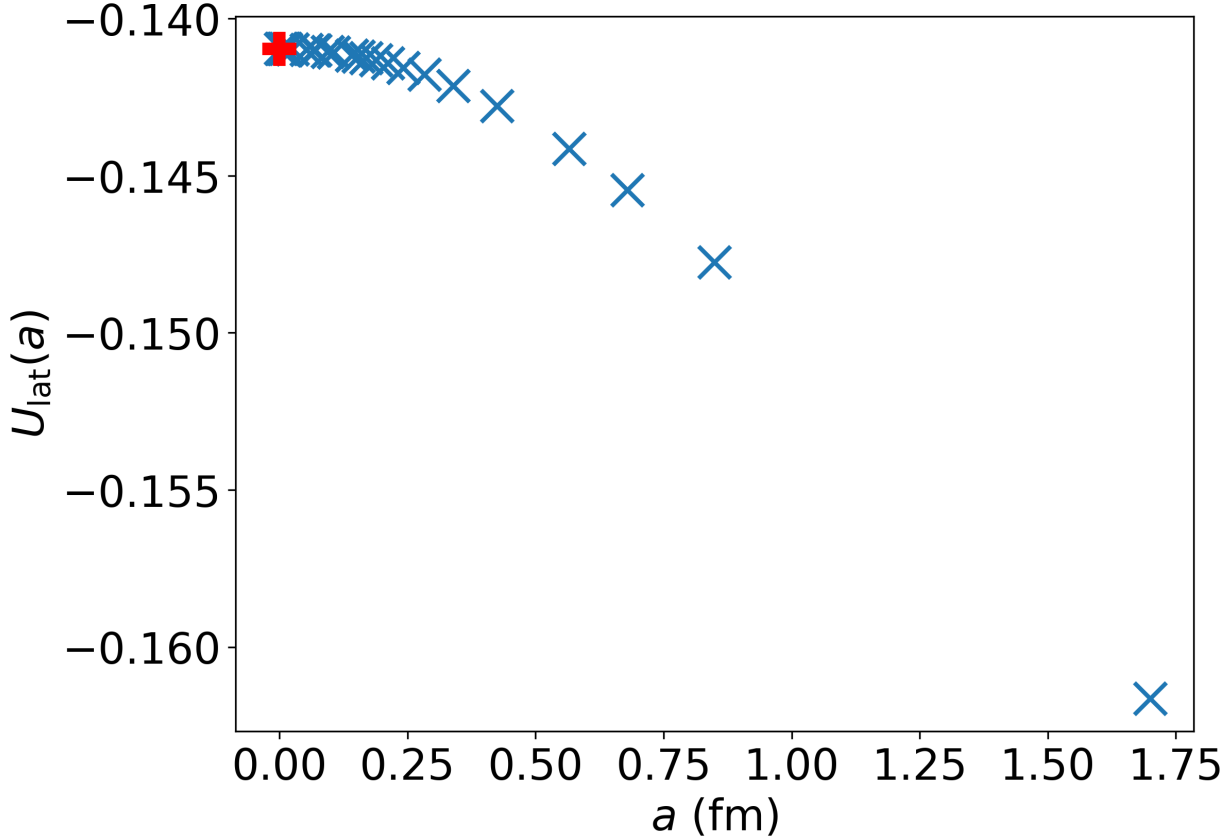


FIG. 3: The plots of $U_{\text{lat}}(a)$ as a function of the lattice spacing. The cross data is obtained from calculating the sum given in Eq. (30) exactly. The red plus symbol is obtained from two different approaches lattice (Eq. (32)) and finite length (Eq. (34)).

Using the same parameters from Table I, we find that $a_1/L_{\text{phy}} = 0.875865$, leading to $U_{\text{F.L.}} = -2/(m_{\text{phy}}a_1) = -0.140966$, which agrees with the value of U_{lat} obtained above. This is not surprising because Eq. (32) is completely equivalent to Eq. (34). When $x < 0$ for the bound state, \sqrt{x} takes a complex value, hence Eq. (36) can be rewritten in terms of the hyperbolic tangent. Once a_1 is fixed, Eq. (34) can be inverted to obtain the corresponding values of x_k for the excited states. These values are then used to compute the excited-state energies via the relation:

$$E_k^{(2\text{B})} = \frac{4\pi^2 x_k}{m_{\text{phy}} L_{\text{phy}}^2}. \quad (37)$$

Applying this method, we find the first few excited-state energies to be:

$$E_{1,\text{F.L.}}^{(2\text{B})} = 124.742 \text{ MeV}, \quad (38)$$

$$E_{2,\text{F.L.}}^{(2\text{B})} = 549.267 \text{ MeV}. \quad (39)$$

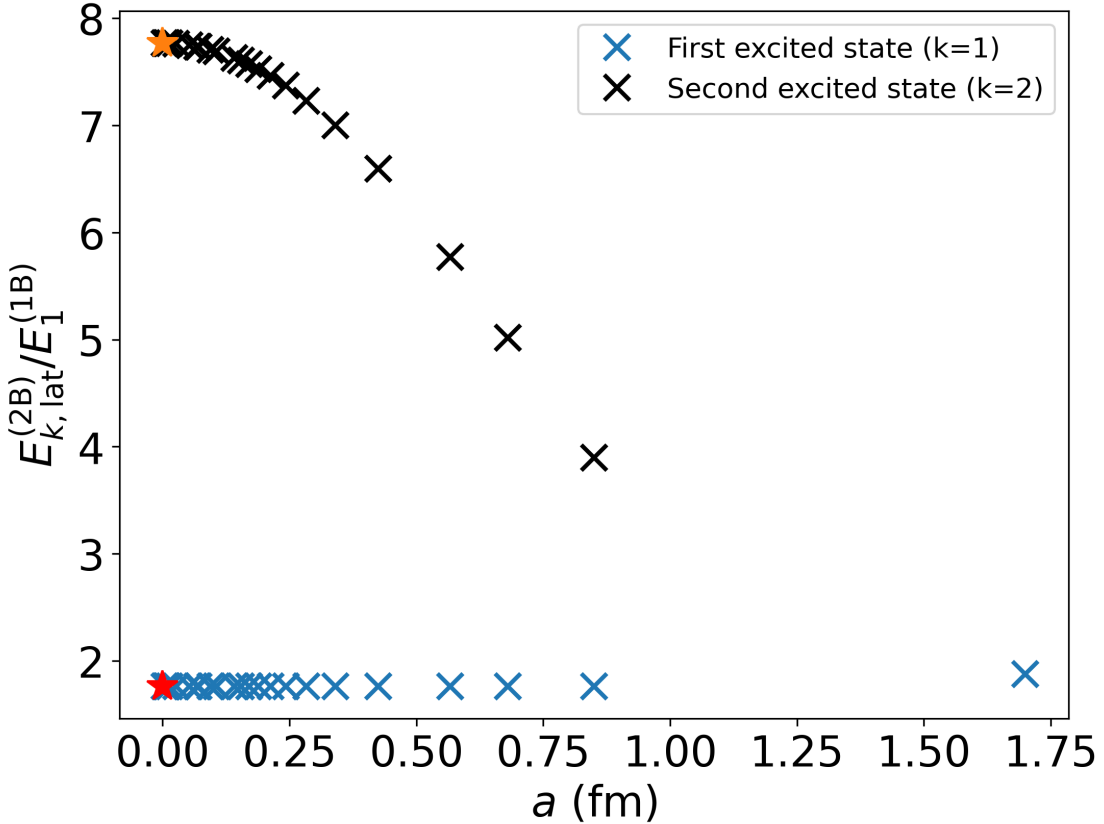
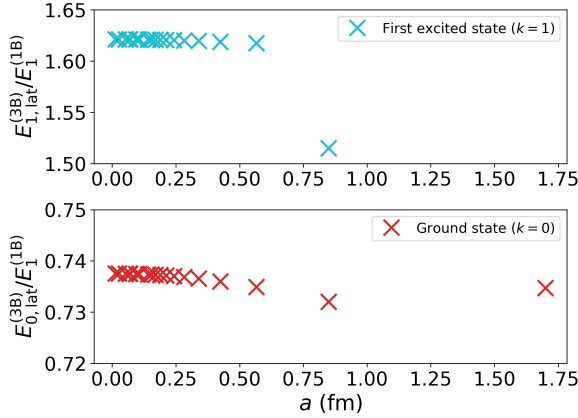


FIG. 4: The plot of the ratio $E_{k, \text{lat}}^{(2B)}/E_1^{(1B)}$ for the two excited states $k = 1, 2$ as a function of the lattice spacing. The star symbols represent their values at the continuum obtained from finite length scheme.

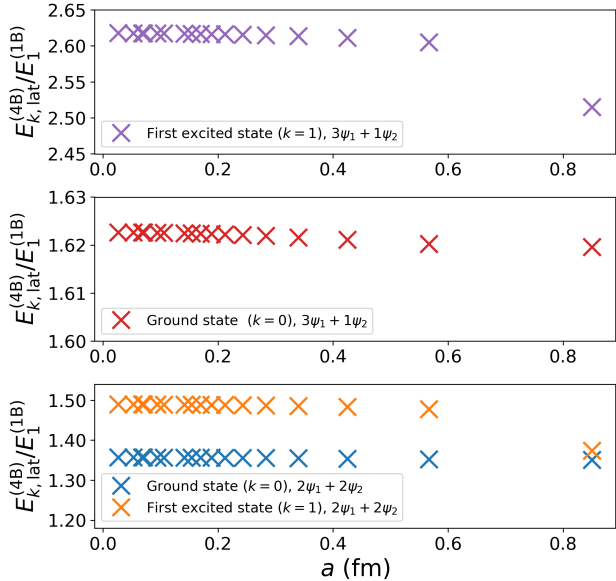
Our computation of the first two excited levels in the two-body system are presented in Fig. 4. In the continuum limit $a \rightarrow 0$, our numerical results converge to the expected values derived from Eq. (34) and Eq. (36).

C. Application in Three- and Four-Body Systems

Using the `Quspin` package, we compute the ground state and first excited state energies of three- and four-body systems. Once the Hamiltonian is constructed, the same numerical framework can be applied to systems with different particle numbers and lattice sizes by simply adjusting the input parameters. The resulting energy spectra for the three- and four-body systems, shown in Figs. 5a and 5b.



(a) The plot of the lowest two energy levels of the three-body system as functions of the lattice spacing. Calculations are performed on lattices of up to 256 sites.



(b) The plot of the lowest two energy levels four-body systems as functions of the lattice spacing. The calculations are performed on lattices of 128 sites due to the increased computational cost.

FIG. 5: Lattice-spacing dependence of low-lying energy levels in the three- and four-body systems.

IV. INFINITE VOLUME EXTRAPOLATION

A. Two-body system

Another important limit of a lattice model is the infinite volume limit⁴¹. At the infinite volume limit, the discretized lattice results is supposed to predict the outcome of an experimental measurement⁴², or a continuous theory. However, this is not guaranteed for every model, as discussed in Ref.³⁹. An example would be the finite-system description of the superconductivity theory. Though it successfully reproduces the spectra of low energy states of many nuclei, this theory fails to approach the normal BCS theory as the system size becomes infinite⁴³. Therefore, we want to test our lattice model at the $L_{\text{phy}} \rightarrow \infty$ limit. To approach the limit, the lattice spacing a is fixed at a small value and the lattice sites L is increased. From Eq. (32) which is valid for $a \ll 1$, if $L_{\text{phy}} \rightarrow \infty$ all exponential terms will

vanish. Also, we have already shown earlier that $U_{\text{lat}}(0) = U = -0.140966$. The two-body energy in the infinite length limit is then given by

$$E_{\infty}^{(2B)} = -\frac{m_{\text{phy}} U^2}{4} = -4.66975 \text{ MeV}. \quad (40)$$

The ∞ subscript indicates infinite-length limit. Since all lattice couplings are known, we can find the spectrum of the Hamiltonian as a function of L_{phy} . The results are presented in Fig. 6.

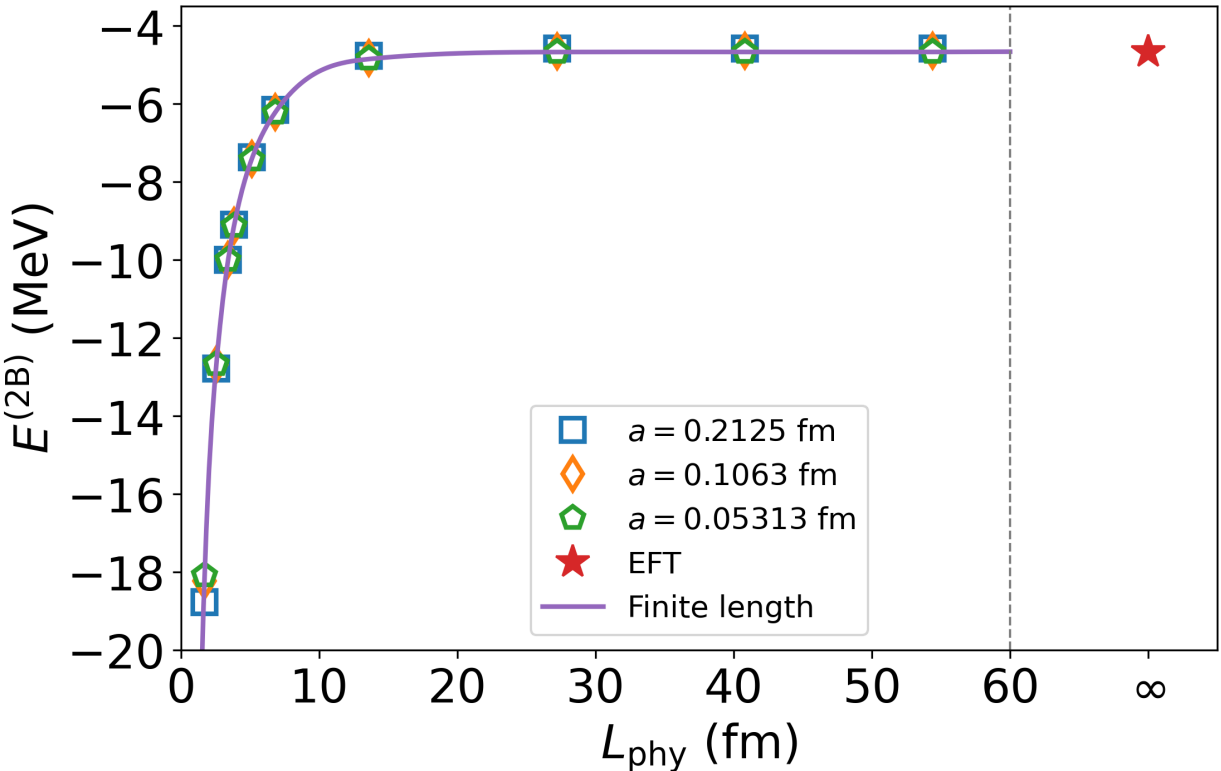


FIG. 6: The plot of ground state energy $E^{(2B)}$ as a function of physical size of the box. The red star indicates the ground state energy of a delta potential quantum system.

To assess discretization effects, we performed calculations at three different lattice spacings. At the largest lattice spacing considered $a = 0.2125 \text{ fm}$, the deviation from the exact value is approximately 2%. The lattice results exhibits an $\mathcal{O}(a^2)$ scaling (see Fig. 7).

We can extract the continuum value $E_{\infty}^{(2B)}$ using the $a = 0.05313 \text{ fm}$ and $2a = 0.1063 \text{ fm}$ data sets via a Richardson extrapolation⁴⁴,

$$E_{\infty}^{(2B)} = \frac{4E_{\infty}^{(2B)}(a) - E_{\infty}^{(2B)}(2a)}{3} = -4.66974 \text{ MeV}. \quad (41)$$

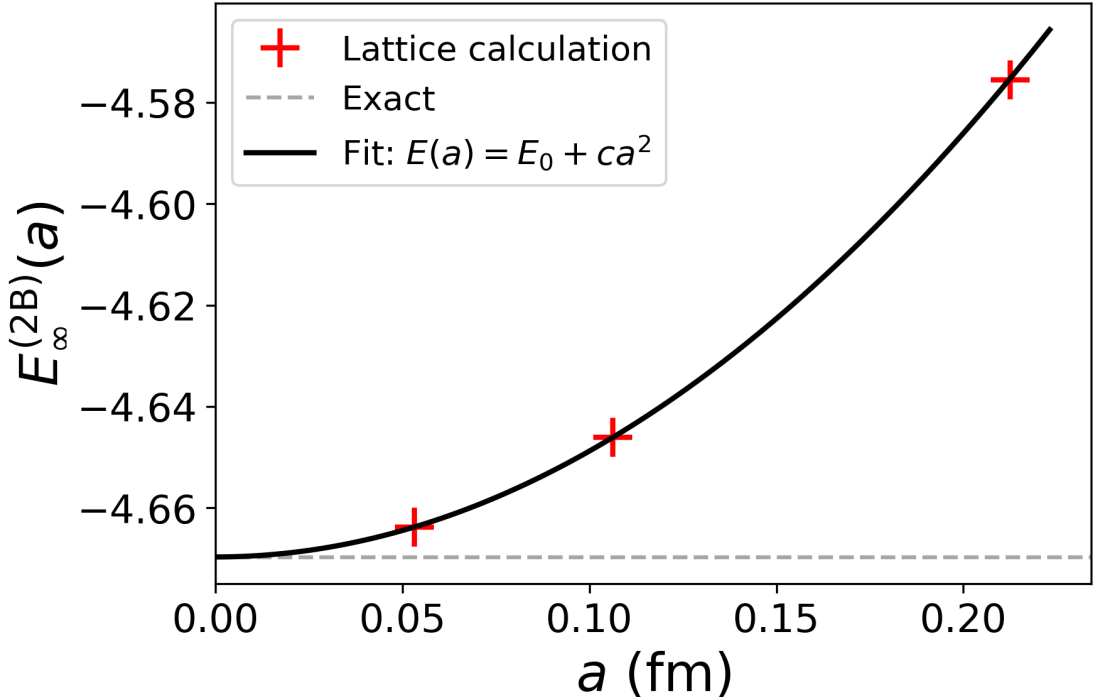


FIG. 7: The plot of extrapolated ground state energy $E_{\infty}^{(2B)}$ in the infinite length limit at three different lattice spacing values. The solid line is a quadratic fit to the data.

The systematic estimate of the discretization effect is

$$\delta_E = |E_{\infty}^{(2B)} - E_{\infty}^{(2B)}(a)| = 0.00592 \text{ MeV.} \quad (42)$$

The two-body sector's ground state energy is reproduced with high accuracy. For comparison, if we use $a = 0.1063$ fm and $2a = 0.2125$ fm instead, the extrapolated two-body binding energy is $E^{(2B)} = -4.6696(236)$ MeV. The uncertainty is increased by a factor of 4.

B. Three-body system

It is straightforward to extend this calculation to a three-body system consisting of two ψ_1 particles and one ψ_2 particle. The dependence of the three-body ground state energy on the box length is shown in Fig. 8. The finite-length ground state energy decreases with increasing L_{phy} and becomes negative for $L_{\text{phy}} \gtrsim 10$ fm. Unlike the two-body problem, a two-body subsystem embedded in a three-body system is strongly affected by finite length quantization of spectator motion. At small box sizes, the increased relative kinetic energy

prevents the formation of a bound subsystem, even though the isolated two-body state is strongly bound.

The finite-size dependence of a bound state is expected to be exponentially suppressed with the system length. This behavior originates from the exponential decay of the bound-state wavefunction outside the interaction region, which leads to an exponentially small sensitivity to the boundaries. Consequently, the leading finite-size correction takes the form $E^{(3B)}(L_{\text{phy}}) = E_{\infty}^{(3B)} + Ae^{-\kappa L_{\text{phy}}}$. Using this functional form to fit our numerical results, we extract the infinite length three-body's binding energy $E_{\infty}^{(3B)}(a = 0.2125 \text{ fm}) = -4.5062(57) \text{ MeV}$ with $L_{\text{phy}} \gtrsim 27.2 \text{ fm}$ and $E_{\infty}^{(3B)}(a = 0.1063 \text{ fm}) = -4.5128(114) \text{ MeV}$ with $L_{\text{phy}} \gtrsim 20.4 \text{ fm}$.

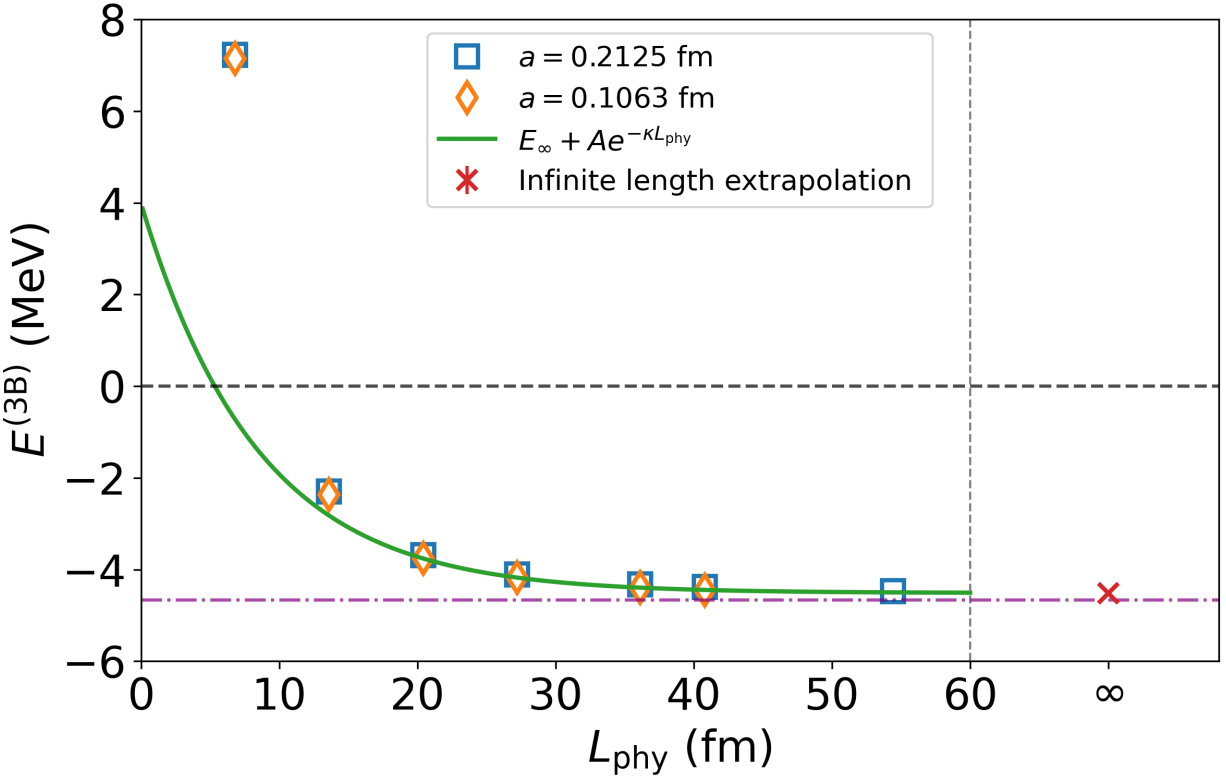


FIG. 8: The plot of three-body system's ground state energy $E^{(3B)}$ as a function of physical size of the box. The dash-dotted line is the $E^{(2B)}$ discussed in Section II. The fitting is performed on $a = 0.2125 \text{ fm}$ data.

If we assume that the $\mathcal{O}(a^2)$ scaling holds for three-body system, the extrapolation of $E^{(3B)}$ in the continuum limit is

$$E_{\infty}^{(3B)}(0) = -4.5150(154)_{L_{\text{phy}} \rightarrow \infty}(22)_{a \rightarrow 0} \text{ MeV}. \quad (43)$$

The continuum-extrapolated three-body energy differs from the two-body binding energy by approximately 0.15 MeV ($\sim 3\%$), well outside the total uncertainty ($\sim 9\sigma$). It should be noted that from the field theoretical perspective discussed in Section II, $E^{(3B)} = E^{(2B)}$. The discrepancy highlights the sensitivity of few-body observables on lattice and finite-length artifacts.

In this calculation, we can go up to $L = 384$ lattice sites. For $a = 0.2125$ fm, the corresponding physical box length is of $L_{\text{phy}} = 81.6$ fm, for which the calculated ground state energy is -4.5281 MeV. This data point is not shown in Fig. 8, but is used as an independent benchmark. It differs from the infinite-volume extrapolation by approximately 4σ despite the large physical size of the box. This indicates that the three-body system has not yet entered the asymptotic finite-length regime. Unlike the two-body sector, the three-body energy involves additional correlations and momentum scales. As a result, residual bias from pre-asymptotic lengths or from the fitting function cannot be excluded. This effect will definitely be exacerbated in the extrapolation using $a = 0.1063$ fm given that exact diagonalization's computational cost limits the accessible lattice spacings and system sizes. We have to reduce the fitting range in order to get the statistical uncertainty. Additionally, the continuum extrapolation is constrained by only two lattice spacings and assumes leading $\mathcal{O}(a^2)$ scaling. Higher-order discretization effects may influence the extrapolated three-body energy, even though such effects are negligible in the two-body sector.

It is worth mentioning that in the two-body sector we were able to reach $L = 1024$ sites (for $a = 0.05313$) thanks to the reduced one-body basis (see Eq. (27)) and the fact that ground state exists in $q = 0$ relative momentum sector. We believe this strategy can be extended for the three-body problem. Any reduction of the three-body basis toward an effective two body would substantially extend the accessible lattice sizes and hence improve the numerical accuracy. We defer such an exploration to future work.

C. Four-body system

The four-body problem in one-dimensional non-relativistic fermion systems with contact interactions presents a qualitatively different level of complexity compared to the three-body case. The lattice formulation plays a central role in the study of the four-body system. By discretizing the Hamiltonian on a finite lattice, the four-body spectrum can be computed

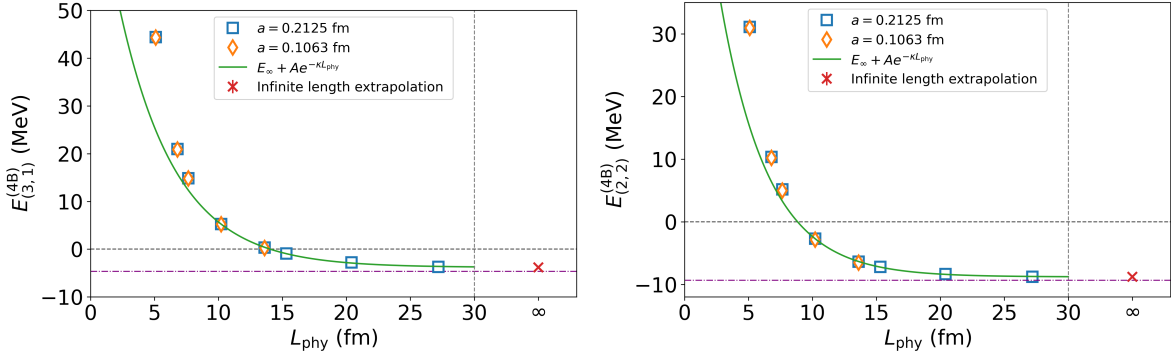


FIG. 9: The plot of four-body system's ground state energies $E^{(4B)}$ as a function of physical size of the box. The subscripts (3, 1) and (2, 2) label the four-body channels by particle content. The dash-dotted line corresponds to $E^{(2B)}$ (left) and $2E^{(2B)}$ (right) benchmarks, respectively. The fitting is performed on $a = 0.2125$ fm data.

non-perturbatively through exact diagonalization. Fig. 9 presents the four-body ground state energies as a function of L_{phy} . They are converging with increasing L_{phy} , but have not yet reached the asymptotic finite length regime.

A detailed analysis of finite-volume and lattice-spacing systematics analogous to the two- and three-body cases is not currently feasible. The four-body results should be treated as exploratory, focusing on qualitative trends rather than an exact lattice prediction. Still, if we assume the same fitting form, we can obtain

$$E_{(3,1)}^{(4B)} = -3.814(127) \text{ MeV},$$

$$E_{(2,2)}^{(4B)} = -8.803(62) \text{ MeV}.$$

The four-body energies remain bounded from below by the relevant two-body thresholds. Specifically, the ground state energy of the 3 + 1 system is bounded by the two-body binding energy, while that of the 2 + 2 system is bounded by twice the two-body binding energy. No additional four-body binding below these thresholds is observed.

V. CONCLUSION

In this paper, we revisit one-dimensional non-relativistic fermion systems with an attractive contact interaction using both field theory and lattice methods. The field theory framework provides analytic control in the continuum, allowing us to study the three-body

problem analytically and the properties of the interaction in few-body systems, renormalization, and scattering amplitudes. The lattice formulation, on the other hand, offers a non-perturbative realization of the same theory, enabling the study of the finite-length effect, lattice artifacts, and few-body spectra in a unified framework. Together, these approaches allow for direct cross-checks between analytic continuum predictions and numerical lattice results.

At infinite volume, the two-body system is a quantum mechanical system with a delta potential and has a well-established solution. The resulting two-body scattering amplitude reproduces the exact quantum-mechanical solution. To extend the analysis to the three-body sector, we introduce an auxiliary field to simplify the equations. We then derive the STM integral equation and study the pole structure of three-body scattering amplitude near threshold. We demonstrate that the three-body system's ground state energy is the same as the two-body binding energy. Therefore no new trimer state exists, which also provides important constraint on the four-body systems.

To approach systems with more particles, we adopt a finite volume lattice formulation, the scalability of which is amenable to numerical implementation. The system is discretized on a lattice and the lattice spacing acts as a regulator. Using the numerical exact diagonalization method, we solve for the energy spectra near the continuum limit for systems with up to four fermions. Finally, we verify a valid infinite-volume extrapolation method by fixing a small lattice spacing and increasing the number of lattice sites. In both the continuum limit ($a \rightarrow 0$), and the infinite-volume limit ($L_{\text{phy}} \rightarrow \infty$), the lattice results for two-body system is consistent with our scattering theory calculation. Three- and four-body systems offer stringent tests for the method. In our analysis, we employ a Lüscher-based finite-volume extrapolation to extract infinite-length results. We find that, even for this simple one-dimensional system, finite-length effects dominate the systematic uncertainties, and discretization errors cannot be neglected.

Because the Hilbert space grows exponentially with system size, the required memory for calculation scales up rapidly. For systems with relatively large sizes, more efficient implementations of the lattice methods are required, such as the quantum Monte Carlo simulations. Quantum Monte Carlo simulations are extremely useful when perturbative techniques begin to fail, especially for quantum chromodynamics problems⁴⁵. However, it is difficult for such algorithms to deal with fermion systems due to the sign problem⁴⁶. Various

algorithms are proposed to solve the issue of 'sign problems', including the constrained path Monte Carlo³⁹, exact fermion Monte Carlo³⁹ and Worldline Monte Carlo simulations^{39,45}.

Nevertheless, exact diagonalization still provides a natural and reliable benchmark for testing numerical methods and algorithms applied to more complex one-dimensional quantum systems. An example of such systems is a one-dimensional few-body system with a pairwise local interaction, whose strength is proportional to the relative velocity of two particles³². In this system, a three-body force may appear^{16,47,48}. It is worth studying the nature of the three-body force within the lattice formulation. Detailed discussion will be covered in our future publication.

ACKNOWLEDGMENTS

S.N. conceived and supervised the project. Z.L. carried out the numerical calculations and data analysis and drafted the manuscript. S.N. guided the interpretation of the results and finalized the discussion. All authors contributed to manuscript revision.

S.N. thanks R. Springer for helpful discussion during the initial phase of the project. We acknowledge the use of AI assistance, specifically ChatGPT⁴⁹, in refining the language and clarity of this manuscript and providing citation to itself, before our final rounds of manual review and revision by all authors. Partial funding for this work was received from the Washington and Lee Lenfest Grant program and the Summer Research Scholars program. This work used Jetstream2 at Indiana University through allocation PHY240288 from the Advanced Cyberinfrastructure Coordination Ecosystem: Services & Support (ACCESS) program, which is supported by U.S. National Science Foundation grants #2138259, #2138286, #2138307, #2137603, and #2138296.

AUTHOR DECLARATIONS

Conflict of Interest

The authors have no conflicts to disclose.

Appendix A: Analytical expression of $I_{\text{lat}}^{(\lambda)}(E, a)$ in the continuum limit

We start from the following equation

$$I_{\text{lat}}^{(\lambda)}(E, a) = \frac{1}{L} \sum_{n=0}^{L-1} \frac{1}{E/2\epsilon(a) - 2[1 - \cos(2\pi n/L)]}. \quad (\text{A1})$$

In the continuum limit, $a \rightarrow 0$ $L \rightarrow \infty$ while $La = L_{\text{phy}}$ is fixed, we can use the Poisson summation formula to simplify the sum as

$$\begin{aligned} & \frac{1}{L} \sum_{n=0}^{L-1} \frac{1}{E/2\epsilon(a) - 2[1 - \cos(2\pi n/L)]} \\ &= \int_0^{2\pi} \frac{dq}{2\pi} f(q) + 2 \sum_{k=1}^{\infty} \int_0^{2\pi} \frac{dq}{2\pi} f(q) \cos(qkL), \end{aligned} \quad (\text{A2})$$

where

$$f(q) = \frac{-1}{2 + m|E|a^2 - 2\cos(q)}. \quad (\text{A3})$$

We also assume that the two-body system has a binding energy of $-|E|$. All integrals are finite

$$I_{\text{lat}}^{(\lambda)}(E, a) = \frac{-1}{2\sqrt{b^2 - 1}} \left[1 + 2 \sum_{k=1}^{\infty} (b - \sqrt{b^2 - 1})^{kL} \right], \quad (\text{A4})$$

where $b \equiv 1 + m|E|a^2/2$. Neglecting terms of order $\mathcal{O}(a^2)$, it follows that

$$\begin{aligned} I_{\text{lat}}^{(\lambda)}(E, a) &= \frac{-1}{2a\sqrt{m|E|}} \left[1 + 2 \sum_{k=1}^{\infty} (1 - \sqrt{m|E|}a)^{\frac{kL_{\text{phy}}}{a}} \right], \\ &= \frac{-1}{2a\sqrt{m|E|}} \left(1 + 2 \sum_{k=1}^{\infty} e^{-k\sqrt{m|E|}L_{\text{phy}}} \right). \end{aligned} \quad (\text{A5})$$

We then use the identity $\sum_{k=1}^{\infty} e^{-kx} = \frac{e^{-x}}{1 - e^{-x}}$ to rewrite the sum as

$$\begin{aligned} 1 + 2 \sum_{k=1}^{\infty} e^{-k\sqrt{m|E|}L_{\text{phy}}} &= \frac{1 + e^{-\sqrt{m|E|}L_{\text{phy}}}}{1 - e^{-\sqrt{m|E|}L_{\text{phy}}}} \\ &= \coth \left(\frac{\sqrt{m|E|}L_{\text{phy}}}{2} \right). \end{aligned} \quad (\text{A6})$$

REFERENCES

¹K. M. O’Hara, S. L. Hemmer, M. E. Gehm, S. R. Granade, and J. E. Thomas, “Observation of a strongly interacting degenerate fermi gas of atoms,” *Science* **298**, 2179–2182 (2002).

²H. Moritz, T. Stöferle, K. Günter, M. Köhl, and T. Esslinger, “Confinement induced molecules in a 1d fermi gas,” *Phys. Rev. Lett.* **94**, 210401 (2005).

³Y.-a. Liao, A. S. C. Rittner, T. Paprotta, W. Li, G. B. Partridge, R. G. Hulet, S. K. Baur, and E. J. Mueller, “Spin-imbalance in a one-dimensional fermi gas,” *Nature* **467**, 567–569 (2010).

⁴G. Pagano, M. Mancini, G. Cappellini, P. Lombardi, F. Schäfer, H. Hu, X.-J. Liu, J. Catani, C. Sias, M. Inguscio, and L. Fallani, “A one-dimensional liquid of fermions with tunable spin,” *Nature Physics* **10**, 198–201 (2014).

⁵A. N. Wenz, G. Zürn, S. Murmann, I. Brouzos, T. Lompe, and S. Jochim, “From few to many: Observing the formation of a fermi sea one atom at a time,” *Science* **342**, 457–460 (2013).

⁶A. Schirotzek, C.-H. Wu, A. Sommer, and M. W. Zwierlein, “Observation of fermi polarons in a tunable fermi liquid of ultracold atoms,” *Phys. Rev. Lett.* **102**, 230402 (2009).

⁷S. Tan, “Energetics of a strongly correlated fermi gas,” *Annals of Physics* **323**, 2952–2970 (2008).

⁸M. Barth and W. Zwerger, “Tan relations in one dimension,” *Annals of Physics* **326**, 2544–2565 (2011).

⁹W.-B. He, Y.-Y. Chen, S. Zhang, and X.-W. Guan, “Universal properties of fermi gases in one dimension,” *Physical Review A* **94** (2016), 10.1103/physreva.94.031604.

¹⁰C.-N. Yang, “Some exact results for the many body problems in one dimension with repulsive delta function interaction,” *Phys. Rev. Lett.* **19**, 1312–1314 (1967).

¹¹M. Gaudin, “Un systeme a une dimension de fermions en interaction,” *Physics Letters A* **24**, 55–56 (1967).

¹²X.-W. Guan, M. T. Batchelor, and C. Lee, “Fermi gases in one dimension: From bethe ansatz to experiments,” *Reviews of Modern Physics* **85**, 1633–1691 (2013).

¹³R. Baxter, *Exactly Solved Models in Statistical Mechanics*, Dover books on physics (Dover Publications, 2007).

¹⁴T. Giamarchi, *Quantum Physics in One Dimension*, International Series of Monographs on Physics (Clarendon Press, 2004).

¹⁵D. Pęcak, A. S. Dehkharghani, N. T. Zinner, and T. Sowiński, “Four fermions in a one-dimensional harmonic trap: Accuracy of a variational-ansatz approach,” *Phys. Rev. A* **95**, 053632 (2017), arXiv:1703.08720 [cond-mat.quant-gas].

¹⁶Y. Sekino and Y. Nishida, “Field-theoretical aspects of one-dimensional bose and fermi gases with contact interactions,” *Phys. Rev. A* **103**, 043307 (2021).

¹⁷V. N. Efimov, “Weakly bound states of three resonantly interacting particles.” Tech. Rep. (Ioffe Inst. of Physics and Tech., Leningrad, 1970).

¹⁸V. Efimov, “Energy levels arising from resonant two-body forces in a three-body system,” *Physics Letters B* **33**, 563–564 (1970).

¹⁹P. F. Bedaque, H.-W. Hammer, and U. van Kolck, “Renormalization of the three-body system with short-range interactions,” *Physical Review Letters* **82**, 463–467 (1999).

²⁰C. Mora, A. Komnik, R. Egger, and A. O. Gogolin, “Four-body problem and bcs-bcs crossover in a quasi-one-dimensional cold fermion gas,” *Physical Review Letters* **95** (2005), 10.1103/physrevlett.95.080403.

²¹J. Wang, H. Hu, and X.-J. Liu, “Hyperspherical Analysis of Dimer-Dimer Scattering in One-Dimensional Systems,” *Few Body Syst.* **66**, 44 (2025), arXiv:2506.01233 [cond-mat.quant-gas].

²²C. Körber, E. Berkowitz, and T. Luu, “Renormalization of a contact interaction on a lattice,” (2020), arXiv:1912.04425 [hep-lat].

²³M. Lüscher, “Volume Dependence of the Energy Spectrum in Massive Quantum Field Theories. 1. Stable Particle States,” *Commun. Math. Phys.* **104**, 177 (1986).

²⁴M. Lüscher, “Volume Dependence of the Energy Spectrum in Massive Quantum Field Theories. 2. Scattering States,” *Commun. Math. Phys.* **105**, 153–188 (1986).

²⁵M. Lüscher, “Two particle states on a torus and their relation to the scattering matrix,” *Nucl. Phys. B* **354**, 531–578 (1991).

²⁶S. R. Beane, P. F. Bedaque, A. Parreno, and M. J. Savage, “Two nucleons on a lattice,” *Phys. Lett. B* **585**, 106–114 (2004), arXiv:hep-lat/0312004.

²⁷R. A. Briceno and Z. Davoudi, “Three-particle scattering amplitudes from a finite volume formalism,” *Phys. Rev. D* **87**, 094507 (2013), arXiv:1212.3398 [hep-lat].

²⁸D. Lee, “Lattice Effective Field Theory Simulations of Nuclei,” *Ann. Rev. Nucl. Part. Sci.* **75**, 109–128 (2025), arXiv:2501.03303 [nucl-th].

²⁹M. G. Endres, “Transdimensional equivalence of universal constants from universal Fermi gases,” *Phys. Rev. Lett.* **109**, 250403 (2012), arXiv:1210.3104 [hep-lat].

³⁰J. E. Drut, J. R. McKenney, W. S. Daza, C. L. Lin, and C. R. Ordóñez, “Quantum anomaly and thermodynamics of one-dimensional fermions with three-body interactions,” *Phys. Rev. Lett.* **120**, 243002 (2018), arXiv:1802.01634 [cond-mat.quant-gas].

³¹Y. Nishida and D. T. Son, “Universal four-component fermi gas in one dimension,” *Phys. Rev. A* **82**, 043606 (2010).

³²S. Y. Yong and D. T. Son, “Effective field theory for one-dimensional nonrelativistic particles with contact interaction,” *Phys. Rev. A* **97**, 043630 (2018), arXiv:1711.10517 [cond-mat.quant-gas].

³³T. G. Backert, F. Brauneis, M. Čufar, J. Brand, H.-W. Hammer, and A. G. Volosniev, “Effective Theory for Strongly Attractive One-Dimensional Fermions,” *Phys. Rev. Lett.* **135**, 040401 (2025), arXiv:2412.05915 [cond-mat.quant-gas].

³⁴D. J. Griffiths and D. F. Schroeter, *Introduction to Quantum Mechanics*, 3rd ed. (Cambridge University Press, 2018).

³⁵J. H. Hetherington and L. H. Schick, “Low-energy $\Lambda - d$ scattering and the hypertriton with separable potentials,” *Phys. Rev.* **139**, B1164–B1169 (1965).

³⁶C. Mora, R. Egger, A. O. Gogolin, and A. Komnik, “Atom-dimer scattering for confined ultracold fermion gases,” *Phys. Rev. Lett.* **93**, 170403 (2004), arXiv:cond-mat/0406627.

³⁷C. Mora, R. Egger, and A. O. Gogolin, “Three-body problem for ultracold atoms in quasi-one-dimensional traps,” *Phys. Rev. A* **71**, 052705 (2005), arXiv:cond-mat/0412225.

³⁸P. Weinberg and M. Bukov, “QuSpin: a Python package for dynamics and exact diagonalisation of quantum many body systems. Part II: bosons, fermions and higher spins,” *SciPost Phys.* **7**, 020 (2019).

³⁹S. Chandrasekharan, S. T. Nguyen, and T. R. Richardson, “Worldline monte carlo method for few-body nuclear physics,” *Phys. Rev. C* **110**, 024002 (2024).

⁴⁰C. Körber, E. Berkowitz, and T. Luu, “Renormalization of a Contact Interaction on a Lattice,” (2019), arXiv:1912.04425 [hep-lat].

⁴¹I. Montvay and G. Münster, *Quantum Fields on a Lattice*, Cambridge Monographs on Mathematical Physics (Cambridge University Press, 1994).

⁴²M. Lenci, “On infinite-volume mixing,” *Communications in Mathematical Physics* **298**, 485–514 (2010).

⁴³E. M. Henley, R. C. Kennedy, and L. Wilets, “Finite superconductors and their infinite volume limit,” *Phys. Rev.* **135**, A1172–A1174 (1964).

⁴⁴L. F. Richardson, “Ix. the approximate arithmetical solution by finite differences of physical problems involving differential equations, with an application to the stresses in a masonry dam,” *Philosophical Transactions of the Royal Society of London, Series A: Containing Papers of a Mathematical or Physical Character* **210**, 307–357 (1911), <https://royalsocietypublishing.org/rsta/article-pdf/210/459-470/307/264773/rsta.1911.0009.pdf>.

⁴⁵H. Singh and S. Chandrasekharan, “Few-body physics on a spacetime lattice in the world-line approach,” *Physical Review D* **99** (2019), 10.1103/physrevd.99.074511.

⁴⁶M. Troyer and U.-J. Wiese, “Computational complexity and fundamental limitations to fermionic quantum monte carlo simulations,” *Phys. Rev. Lett.* **94**, 170201 (2005).

⁴⁷T. Cheon and T. Shigehara, “Realizing discontinuous wave functions with renormalized short-range potentials,” *Physics Letters A* **243**, 111–116 (1998).

⁴⁸T. Cheon and T. Shigehara, “Fermion-boson duality of one-dimensional quantum particles with generalized contact interactions,” *Phys. Rev. Lett.* **82**, 2536–2539 (1999).

⁴⁹OpenAI, “Chatgpt,” <https://chat.openai.com/> (2023), accessed: 2026-01-02.